UCRL-JC-126746
PREPRINT

LLNL's Acoustic Spectrometer

John Baker

This paper was prepared for submittal to the
Peace and Wartime Applications and Technical Issues for Unattended Ground Sensors
Orlando, FL
April 21-25, 1997

March 17, 1997

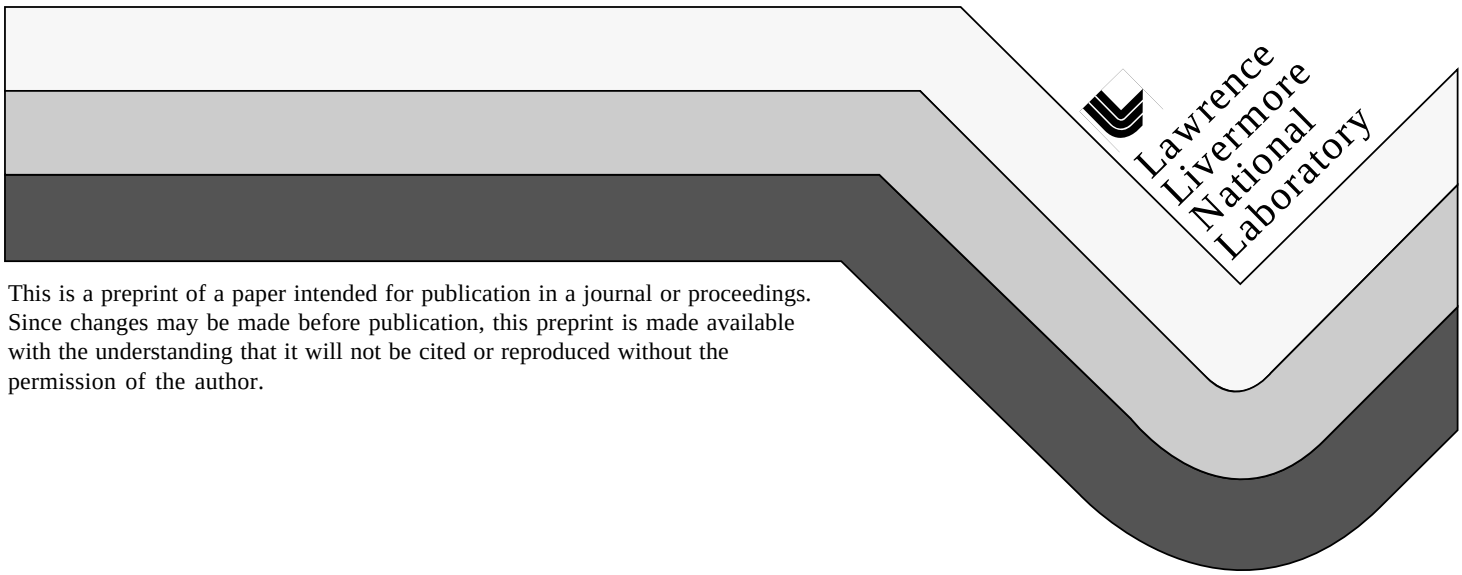

LLNL's acoustic spectrometer

John Baker
Lawrence Livermore National Laboratory, MS L-183, P.O. Box 808, Livermore, CA 94550

ABSTRACT

This paper describes the development of a frequency sensitive acoustic transducer that operates in the 10 Hz to 10 kHz regime. This device uses modern silicon microfabrication techniques to form mechanical tines that resonate at specified frequencies. This high-sensitivity device is intended for low-power battery powered applications.

Keywords: Sensor, acoustic, micromachined, spectrometer, low-power, unattended, test, portable.

1. INTRODUCTION

In 1991, the Sensor Application Group (SAG) at LLNL began development of acoustic sensors, the LLNL Acoustic Spectrometers, for use in detection and spectral analysis of vibration and acoustic (sound) signals. The first sensor, a fiber optic device using 24 fibers primarily for multichannel detection and analysis of vibrational signals, was developed under internal LLNL R&D funding. Subsequent devices developed under U. S. Department of Energy (DoE) and ARPA contracts have utilized micromachining technology to produce more sensitive and smaller sensors for application as acoustic or vibration detectors and analyzers. The sensors consist of an array of a large number of mechanically resonant tines micromachined on three-inch diameter silicon wafers at the LLNL Microtechnogy Center. These sensors have particular advantages over a single microphone or geophone type sensor followed by a digital processing unit, specifically freedom from jamming by a single or a few interfering signals and potentially very low power operation. The challenges have been to 1) perfect the fabrication procedures to assure adequate tine array yield and 2) to develop a miniature low-power multichannel readout device to measure the vibration amplitude of the micromachined tines, producing acoustic spectra from the sensors and thereby realize the promise of the micromachined device.

2. INITIAL FIBER-OPTIC ACOUSTIC SPECTROMETER DEVELOPMENT

The LLNL Acoustic Spectrometer development project began with a fiber optic device in 1991 to detect and provide spectral analysis of vibration and/or acoustic signals, supported by internal LLNL R&D funding, developed under the direction of Dr. Sang Sheem. The first application was to be detection of the vibration of rotating machinery such as manufacturing equipment, pumps, motors and other equipment. As a proof of concept, the first device used an array of twenty-four mechanically resonant 125 μm diameter cantilevered glass fibers of various lengths supported on an aluminum plate. A sketch of this first early fiber-optic Acoustic Spectrometer device is shown in figure 1. Readout of the vibration amplitude of the vibrating tines was by use of a CCD array to detect the laser beams emanating from the glass fibers.

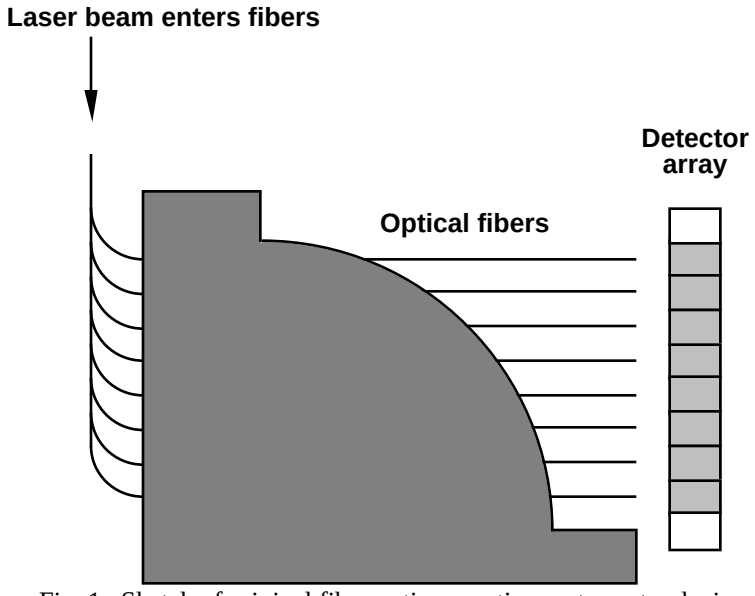

Fig. 1. Sketch of original fiber optic acoustic spectrometer device

As an accelerometer, this first device had a sensitivity of approximately 5 mm per g at a frequency of 100 Hz, dropping off at higher frequencies at a rate of approximately $f^{1.5}$. The frequency range of the fiber-optic device was 100 Hz to 1100 Hz and the glass fibers had a bandwidth of approximately 1.5 Hz at 100 Hz increasing to a bandwidth of 7 Hz at 1100 Hz. A frequency response graph for the fiber optic acoustic spectrometer is shown in figure 2, where the frequency range and narrow bandwidth of the individual tines are evident. Although not particularly sensitive, this first sensor demonstrated that the spectra of vibrational signals could be measured, encouraging sponsorship by the DoE of a more sensitive device using micromachining technology.

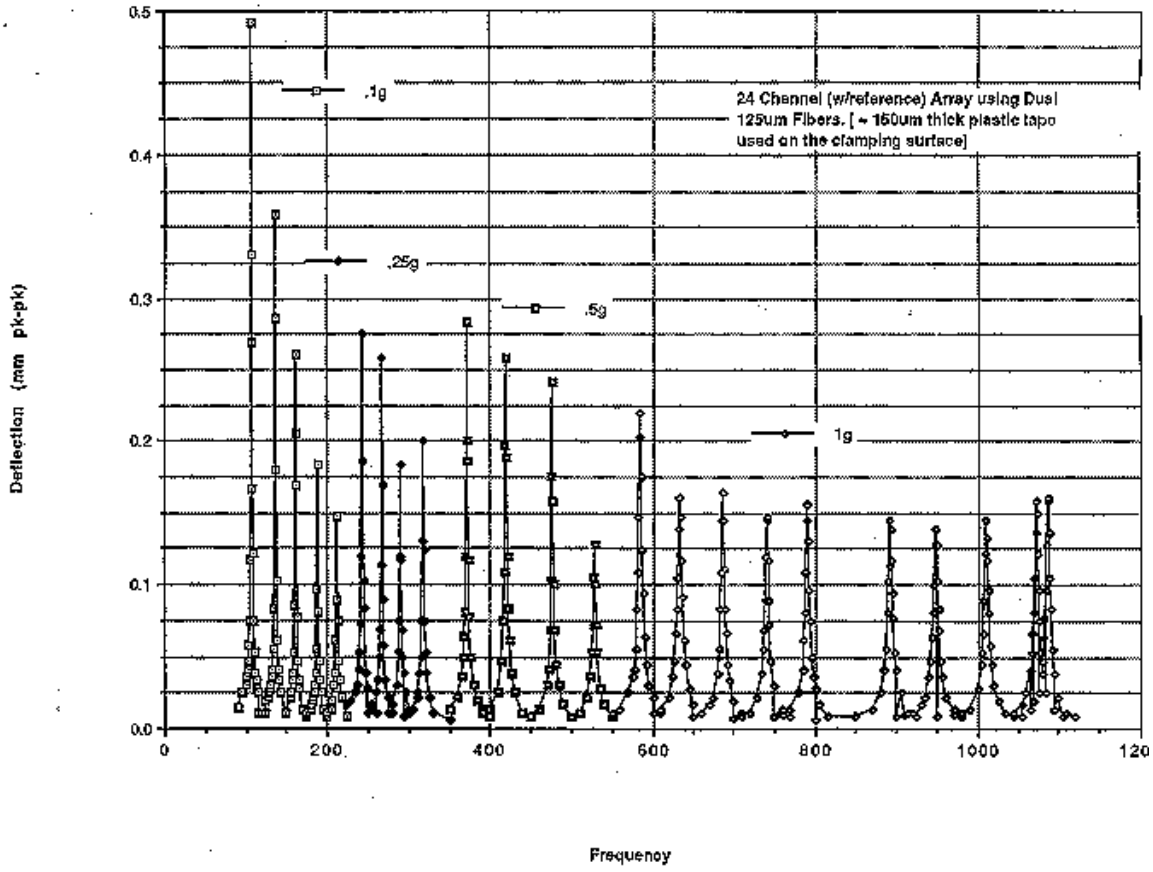

Fig. 2. Frequency response of original fiber-optic acoustic spectrometer device.

3. MICROMACHINED ACOUSTIC SPECTROMETER DEVELOPMENT

In order to realize the high accuracy and miniature size afforded by micromachining technology, silicon micromachining was chosen for future LLNL acoustic devices and the SAG began development of a micromachined acoustic spectrometer device in 1994 under DoE sponsorship, with Sang Sheem continuing as the P. I. for the project. ARPA joined DoE in sponsoring development of the micromachined devices with interest in applying the sensor as a low-power high-sensitivity wake-up device and spectrometer for other higher power sensors in a sensor package.

3.1 Micromachined silicon tine arrays

SAG designed and fabricated four micromachined tine arrays, etched on 3-inch diameter, 300 μm thick silicon wafers. Cantilevered beams were chosen for the acoustic spectrometer devices as previous work had indicated a serious problem with multiple vibrational modes when the beams were held at both ends. The tines ranged in length from 0.3 cm for the 3 kHz tine to 5.5 cm for the 10 Hz tine. A photo of one of the arrays, a 64 tine array designed for detecting acoustic frequencies between 43 Hz and 232 Hz, is shown in figure 3. On this array, the tine lengths range from 0.85 cm to 1.9 cm. The tines are cantilevered from the wafer near the center of the photo.

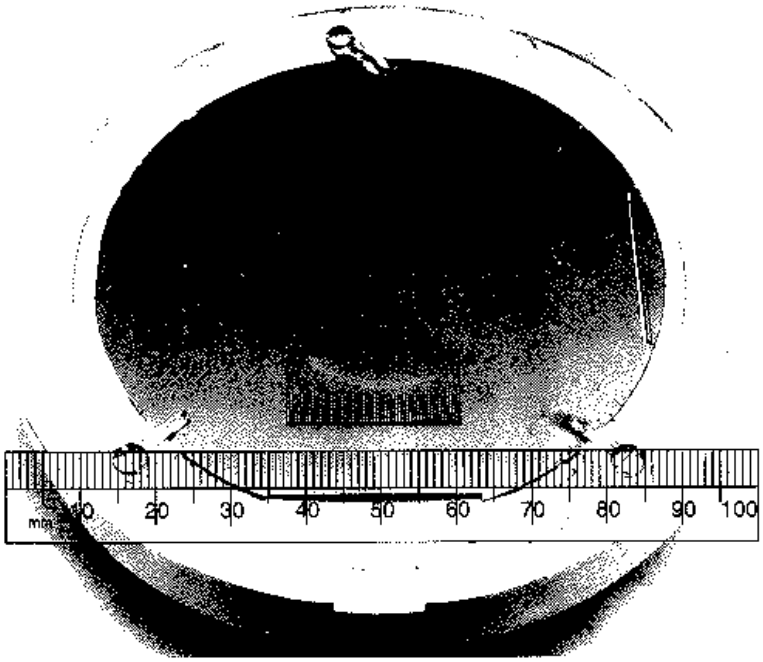

Fig. 3. Micromachined 64 tine silicon tine array designed for 43 Hz to 232 Hz.

Other arrays were designed to cover the range of 10 Hz to 40 Hz, 242 Hz to 872 Hz and 907 Hz to 3.112 kHz. The 10 Hz to 40 Hz array used 16 tines while the other arrays used 64 tines. Each tine was to be etched to a thickness of approximately 25 μm from the 300 μm thick wafer. However, measurement of the finished wafers showed that the tines were etched to a thickness of approximately 35 μm, raising the resonant frequencies by a factor of two. Warping and sagging were a particular problem, particularly with the longer tines, amounting to nearly a millimeter when the array was held horizontally.

3.2 Optical spectrometer tine amplitude readout

Optical interferometry was chosen to provide a high sensitivity readout of the tine vibration. Piezoresistive and capacitive measurement techniques were considered and rejected as not providing the ultra-high sensitivity that we concluded was needed for the wake-up sensor application. Both analog readout providing better than 1/100 wavelength sensitivity and fringe counting were planned and a laboratory prototype instrument was designed and built to accommodate two of the micromachined tine arrays in the Michelson interferometer configuration. A tunable 30 mW solid-state laser operating at approximately 690 nm with beam-forming optics provided a line beam for illuminating the ends of the tines. Electronics circuitry using a 75 element Hamamatsu photodiode array was designed for use with system and tests were conducted to characterize the arrays. A photo of the laboratory prototype is shown in figure 4 below. The laser is shown in the lower left of the photo with the two arrays and associated electronics at the upper right. Micrometer adjustable mounts supported the two arrays and the electronics. The overall dimensions of the prototype are approximately 30 cm x 30 cm x 30 cm.

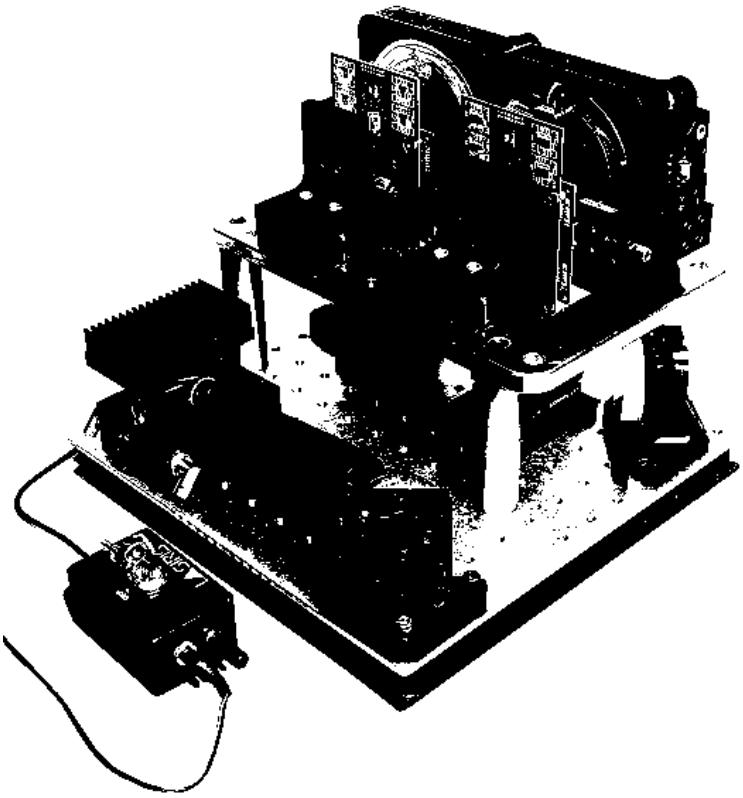

Fig. 4. Photo of the laboratory prototype acoustic spectrometer

3.3 Tine array characterization

The laboratory prototype was placed in a small 0.6 m x 0.6 m x 1.2 m Acoustics Systems Inc. acoustical chamber for testing and characterization of the two tine arrays. Signals from a Hewlett-Packard function generator were amplified to power a loudspeaker. The audio signal levels were monitored with a laboratory quality Bruel & Kjaer Instruments microphone. It was not possible to align all 64 Michelson interferometers simultaneously because of warping in the longer tines. Consequently, testing was conducted on a single tine at a time, requiring time consuming alignment of the apparatus before a frequency response test could be conducted. This is the most serious problem with the optical readout design we had chosen, leading us to reconsider other designs such as piezoresistive and capacitive measurement of the tines' vibration amplitudes.

However, we were able to complete the characterization of the 64 tines of a single array, the array designed for the range of 10 Hz to 40 Hz. Typical spectral response of the tines is shown in figure 5, showing the vibration amplitude in fringe counts along the vertical axis and the frequency in Hz on the horizontal axis. The measured frequency response of the tines shows that the actual frequencies were approximately double the design values, implying that the tines were not etched as thinly as desired or approximately to a thickness of 35 μm instead of the designed value of 25 μm. For these tine characterization tests the sound amplitude was approximately 50 dB SPL but was not held constant over the frequency range. However, the sound amplitude was measured and recorded so that the data could be corrected for amplitude variations. Clearly evident are the sharp peak at about 65 Hz and significant nearby peaks that were identified as resonant peaks of adjacent tines. The adjacent peaks are obviously a serious problem, limiting the sensitivity of the sensor. Subsequent testing of a model, described below, and finite element analysis of the structure indicate that the adjacent peaks are the result of viscous (air) coupling between the tines and not the result of mechanical vibrations through the array structure.

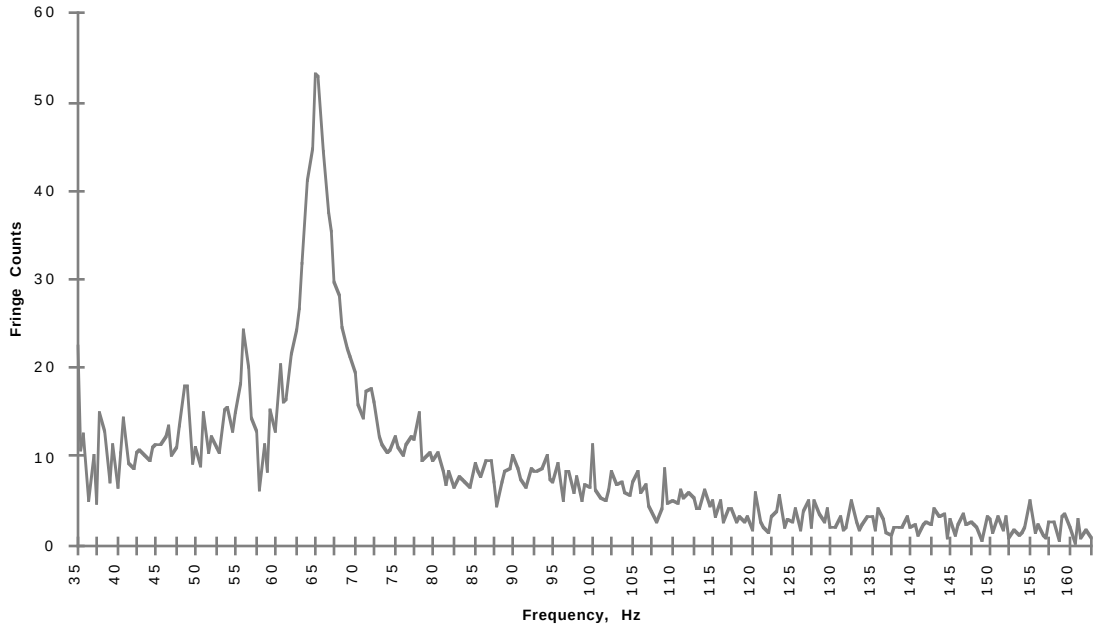

Fig. 5. Frequency response of a typical tine

Also evident in figure 5 is the narrow bandwidth of the tine, approximately 4 Hz in the case of tine #1 shown above. The narrow bandwidth indicates little damping and relatively high sensitivity. A graph of the bandwidth of the tines in figure 6 below shows that the bandwidth is fairly constant at about 3 Hz over the frequency range of the tine array except for the very low frequencies where the effectiveness of the acoustical chamber is poor and the data are suspect.

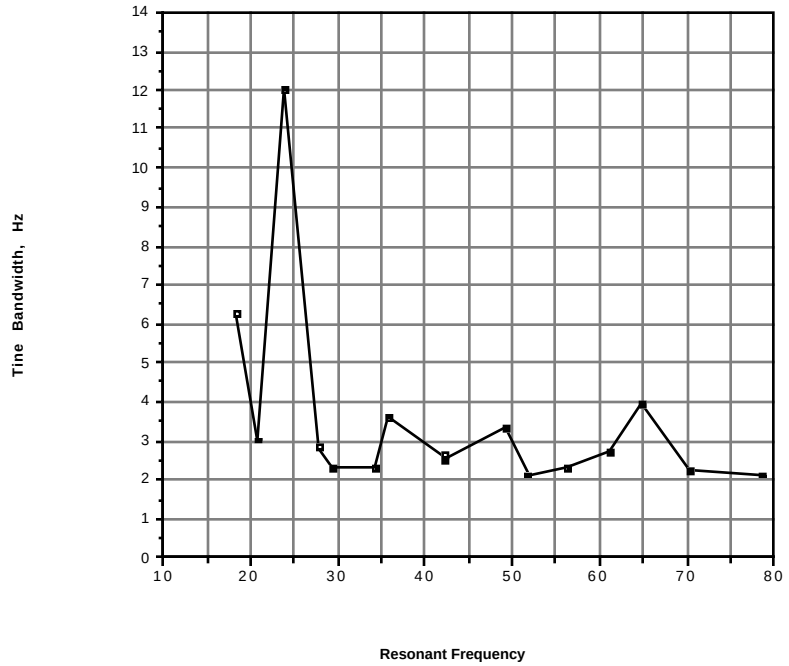

Fig. 6. Measured tine bandwidth of the 10 Hz to 40 Hz tine array

In general terms, the results of the tine characterization tests show the following:

1. Tine frequency response is approximately double the designed value.
2. Sensitivity is relatively high.
3. Bandwidth is fairly constant at approximately 3 to 4 Hz.
4. High adjacent peaks are evident on the frequency response graphs, seriously reducing the tine sensitivity.
5. Alignment of the Michelson interferometers on the laboratory prototype was not possible for all 64 tines of an array simultaneously because of warping and sagging of the tines.

4. CAPACITIVE TINE AMPLITUDE READOUT (CTAR)

Although providing very high sensitivity, the optical interferometry readout technique was shown to be impractical because of the warpage and sagging of the cantilevered tines. Consequently other readout techniques, such as capacitive and piezoresistive methods, were reconsidered. Capacitive readout was selected as we believed that it might be capable of providing the higher sensitivity of the two techniques. Calculations of the capacitance of the tines spaced 300 μm from a pickup electrode, neglecting fringing, would range from 0.027 pF to 0.5 pF and we believed that we could detect capacitance changes of less than 0.001 pF using lock-in amplifier techniques. To test the capacitive readout technique we set up a model using spring-steel, 12 inch long scales.

4.1 CTAR model tests

The model uses 12" long spring steel scales, approximately 1/2" wide. A 6" long scale was used as the electrode in most tests. In later tests we replaced the 6" scale with a 5" x 19" aluminum chassis plate to determine the effectiveness of a larger electrode. Tests conducted with the lowest frequency micromachined silicon tine arrays indicate the amplitude of the tine vibration is a few μm at 50 dB SPL. Tests were conducted with the appropriate scale-to-electrode spacing to give capacitance's in the range of 0.05 pF to 5 pF, similar to the capacitance that were expected in the micromachined device. However, measurements of the model's tine to electrode capacitance gave generally higher values of capacitance that we attributed to fringing effects. A second 12" spring steel scale was added for tests to determine the capacitive coupling between tines and to determine the "air-coupling" or viscosity effects between tines. An oscilloscope with a 10 pF 10X probe was used to detect the electrode signal for capacitance measurements. An AC carrier signal at 40 kHz was selected as the carrier signal, much higher than the highest acoustic signal expected. For signal detectability tests, an EG&G Lock-in Amplifier was used as a synchronous detector to remove the 40 kHz signal and detect a sine-wave signal at the resonance of the steel scales.

4.1.1 Model capacitance measurements

The graphs below in figures 7 and 8 are representative of capacitance tests with the CTAR model using the spring steel scales. The capacitance was approximated by detecting the 40 kHz signal on a 10 pF oscilloscope probe attached to a Tektronix 2440 oscilloscope. The capacitance of the probe was not measured but is specified by the manufacturer. In these capacitance tests, the scales were parallel and facing but were slid longitudinally to vary the overlap between the 6" and the 12" scales. Note that the measured capacitance was always higher than calculated assuming a parallel plate model. We attributed the difference to fringing effects. Using a 10 V pk-pk signal at 40 kHz, the detected signals ranged from approximately 250 mV pk-pk to 600 mV pk-pk.

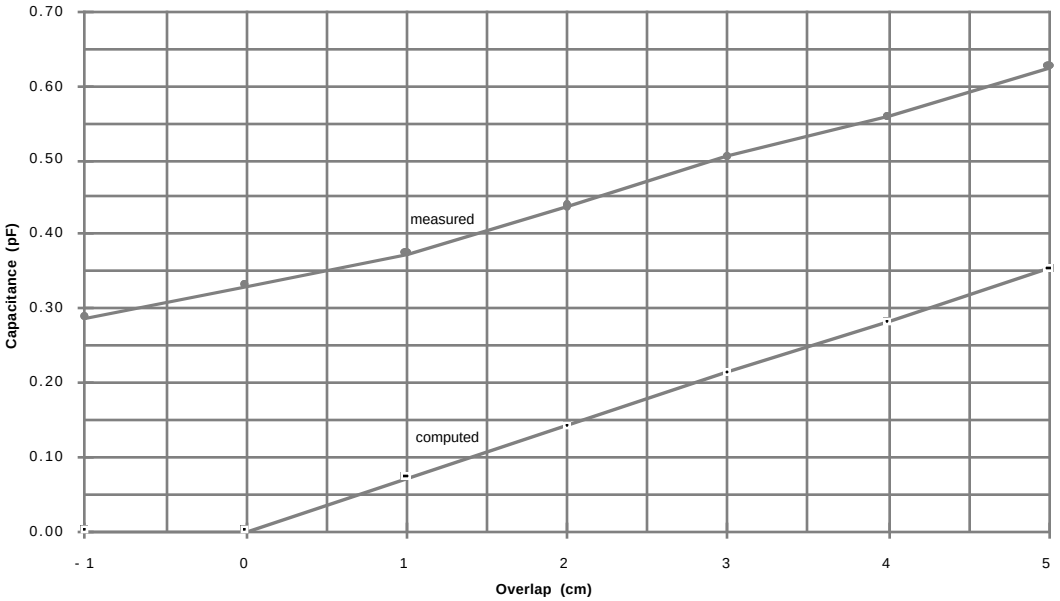

Fig. 7. Model measurements of tine to electrode capacitance, 1.5 cm spacing.

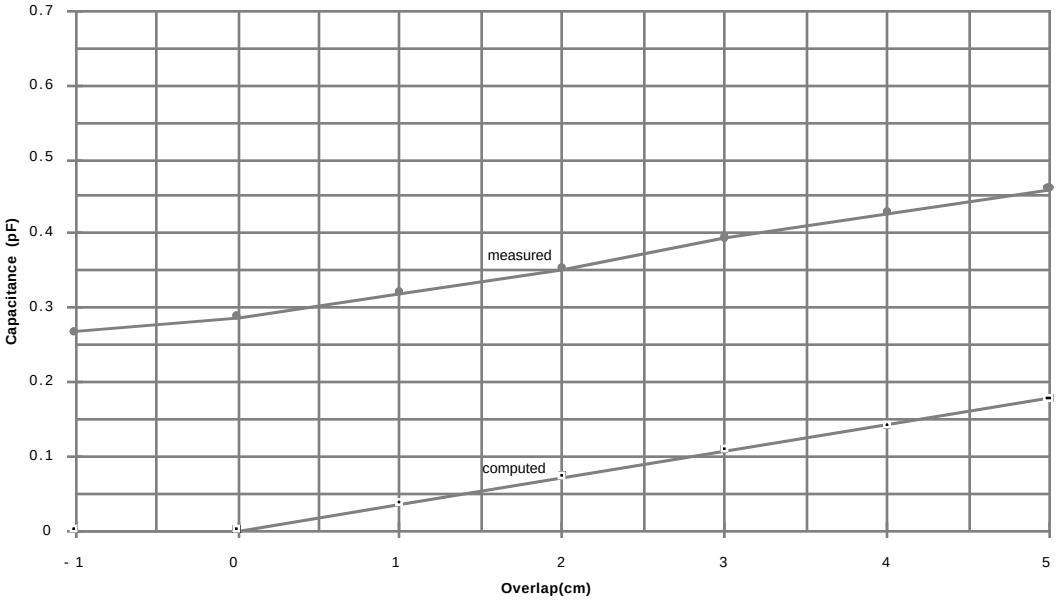

Fig. 8. Model measurements of tine to electrode capacitance, 3 cm spacing.

4.1.2 Model sensitivity and detectability

Sensitivity tests were conducted using the EG&G Lock-in Amplifier. The noise level at the lock-in amplifier output was approximately 5 mV pk-pk. The scales were spaced 5 cm apart for a parallel-plate capacitance of 0.2 pF. For an end-deflection of 1 cm, the lock-in amplifier produced a DC output voltage of 10 V indicating a sensitivity of 10 V/cm = 1 mV/μm. With a noise floor of 5 mV, the minimum detectable deflection is computed to be 5 μm for the model.

Further testing by deflecting the end of the tine +/- from the rest point, the detected 40 kHz signal at the electrode was used to produce the "measured" capacitance shown in the graph below in figure 9. The computed graph assumes a parallel

movement of the tine rather than deflection at the tip and bending of the tine and therefore the slope of the curves differs slightly, the computed graph having a larger slope. The vertical displacement of the two curves probably results from parasitic capacitance to shield plates installed to minimize 60 Hz pickup. Also note that the curves are nonlinear as the capacitance is inversely proportional to the spacing. At zero deflection, the slope is approximately 0.045 pF/cm or 45 fF/cm.

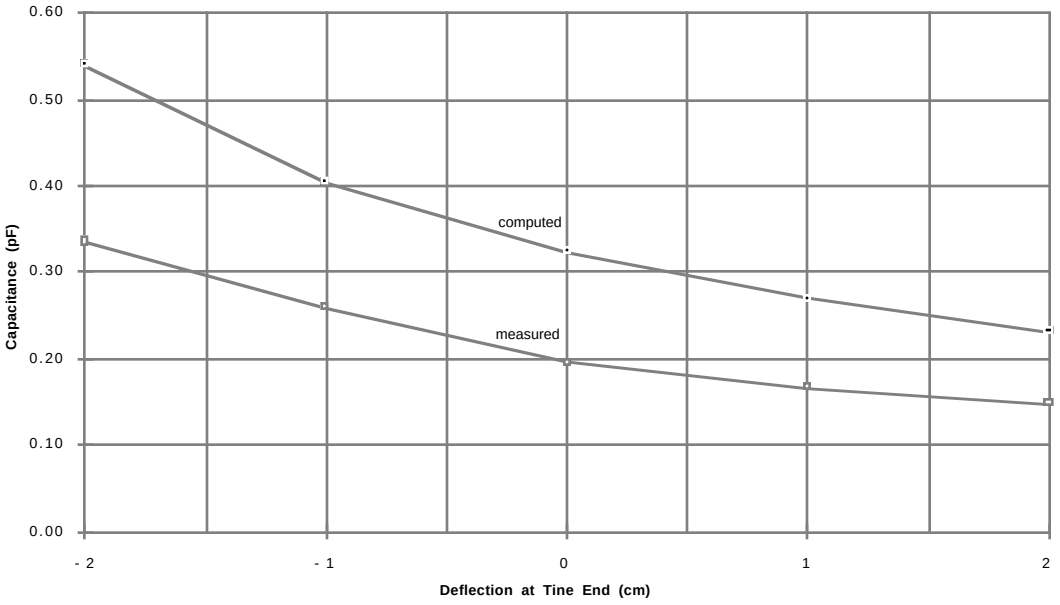

Fig. 9. Model measurements of capacitance change vs. deflection of tine-end.

Computing a minimum detectable change in capacitance, the measured capacitance changed 0.06 pF for the 1 cm deflection mentioned above for which the EG&G output voltage changed 5 V DC. Therefore, using the EG&G lock-in amplifier, the measurement sensitivity is 5 V/0.06 pF = 83.3 V/pF and the minimum detectable capacitance change is:

minimum detectable capacitance change = 0.06 pF x 5 mV / 5 V = 0.06 fF.

Extrapolating to the micromachined tines and assuming a tine to electrode spacing of 300 μm, the minimum detectable deflection is approximately 1/300 of the tine to electrode spacing. For the shortest micromachined silicon tine at 3 mm:

Tine capacitance ≈ e A/d
≈ 8.85 pF * 300 μm * 3 mm / 300 μm = 0.027 pF.

Therefore the minimum detectable deflection is 1/450 times the capacitance of the shortest micromachined silicon tine:

0.06 fF/ 0.027 pF = 1/450.

4.1.3 Air coupling between tines

Visual tests were conducted with the spring-steel tines to investigate the viscous (air) coupling between tines. In the first tests, two 12" spring steel scales were spaced laterally at various distances. One of the scales was set into vibration at its resonant frequency of approximately 4.5 Hz and the effect on the adjacent scale was visually observed. Although only visual, the results appear to be consistent. The graph below in figure 10 shows that the coupling is very strong for spacing less than 1/2 the width of the scales and follows a nearly linear curve from 1/6 the scale width to 1/2 the width indicating that the scales should be spaced more than 1/2 their width in order to minimize the viscous coupling. In a subsequent air coupling test, the effective length of the adjacent tine was varied and the coupling was visually observed between it and the vibrating resonant tine. The results shown in the graph in figure 11 below indicate that the coupling drops off to nearly zero as the ratio of scale lengths is reduced to 0.8:1. Therefore the tine lengths in the array should be alternated to minimize the coupling.

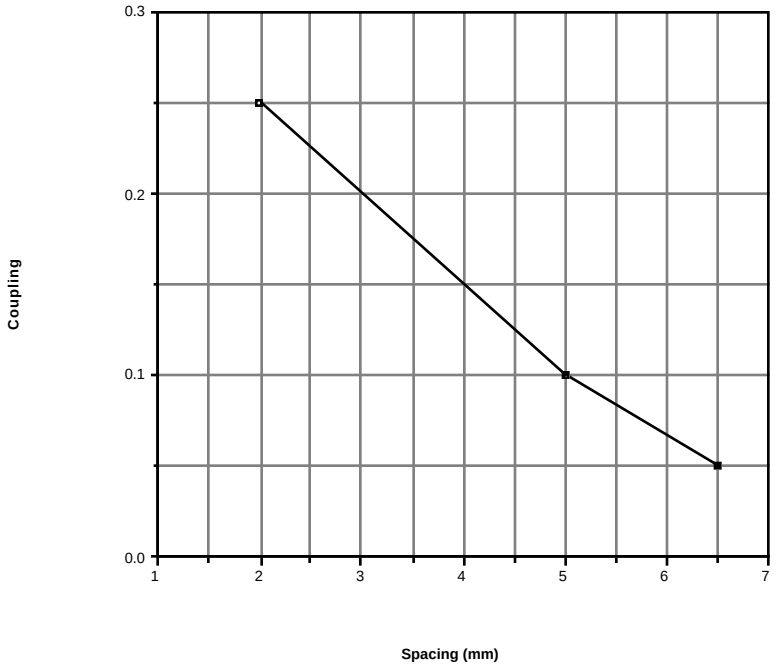

Fig. 10. Viscous (air) coupling between adjacent tines of the same length.

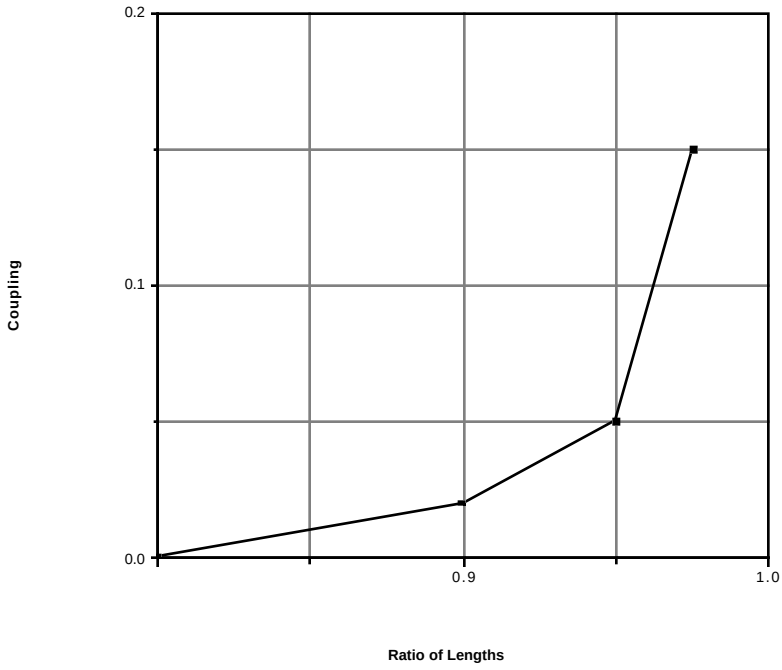

Fig. 11. Viscous (air) coupling between adjacent tines of differing length

4.1.4 Model test conclusions

The main conclusion from the tests with the CTAR model using spring-steel scales was that the capacitive technique using an audio oscillator frequency around 40 kHz appears to be a viable method for measuring the vibrational amplitude of the silicon micromachined tines. Measurement sensitivity is approximately 0.06 fF using a good quality lock-in amplifier, or 1/450 of the computed parallel plate capacitance of the shortest micromachined tine. Other test results show that the tines should be separated by greater than 1/2 their width and that the tine lengths should be alternated to minimize coupling between adjacent tines.

4.2 CTAR micromachined tine array module tests

To further test the CTAR concept, we developed a prototype CTAR module using an existing micromachined tine array, an array designed for 43 Hz to 232 Hz, modified by the addition of metallizing to provide means for connecting to circuitry on adjacent printed wiring boards (PWB's). A sandwich-like module was developed with the 40 kHz drive circuitry on the front PWB, the metallized tine array wafer in the middle and the detection circuitry on the rear PWB. The CTAR block diagram is shown in figure 12.

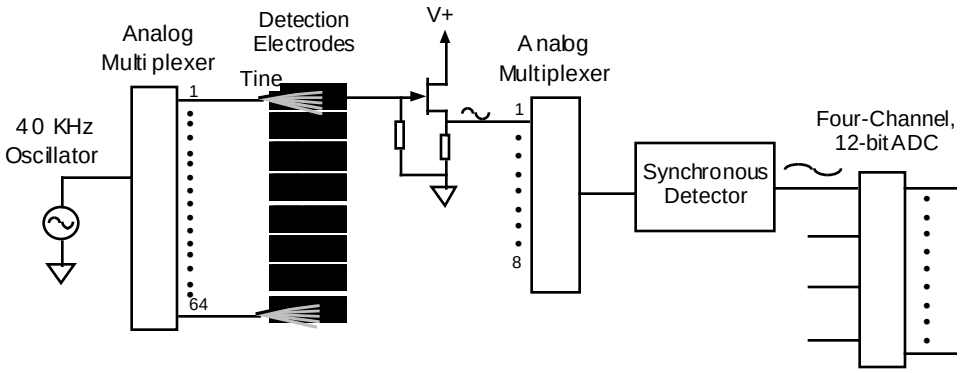

Fig. 12. Block diagram of the CTAR acoustic spectrometer.

4.2.1 Design of the CTAR prototype module

The metallized micromachined silicon tine array was sandwiched between two PWB's containing the necessary electronics circuitry to develop and apply a 40 kHz sine-wave signal individually to the metallized tines on one PWB and to "pick-up" the signal from plated electrodes and derive voltages indicative of the tine-to-electrode capacitance's on the second PWB. The metallized tine array was mounted on a PWB that also included the plated electrode pick-ups, buffer amplifiers, analog multiplexers, lock-in amplifier and peak detector circuitry. Gold metallization of the silicon wafer and tine array was preceded by a coating of silicon nitride in an attempt to isolate the metallized tines from one another. The front PWB comprises the 40 kHz oscillator circuitry, multiplexers to individually select the tines and an elastomeric connector to couple the 40 kHz sine-wave signal to the metallized silicon wafer. A photo of the completed CTAR module follows in figure 13 showing the front PWB on the top with the electrode module supporting the metallized silicon wafer in the middle and a power supply module on the bottom.

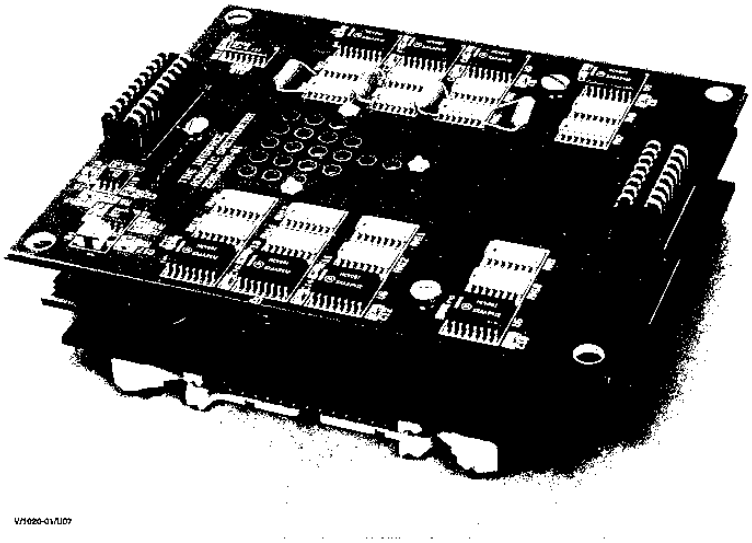

Fig. 13. The completed CTAR test module.

4.2.2 CTAR module test results

Testing of the CTAR module used the same equipment as during testing of the optical interferometry module described above in section 3.3. The results of the tests were inconclusive because of design errors in the electronics modules and because of problems with some of the tines sticking to the pick-up electrodes. However, the measured tine frequency response for the CTAR module exhibited response similar to the optical module but at much poorer sensitivity and with increased interference/crosstalk from adjacent tines. We believe that the electronics design errors led to the poor sensitivity. Since the tests, several electronics design errors have been detected and corrected but follow-up tests have not been conducted. The increased interference from adjacent tines had been expected because of the proximity of the adjacent tines and the relatively high capacitance between adjacent tines. We believe that the "sticking problem" resulted from incomplete metallization of the tines leading to build-up of charge and electrostatic potentials. A graph of the frequency response of one of the tines is shown in figure 14 below. Note that only the nearby frequencies are shown in this particular graph and that high peaks from adjacent tines were observed in other tests. This graph shows considerable broadening of the peak that we attribute to capacitive and viscous coupling from adjacent tines. Overall, we are encouraged by the results of the CTAR module tests as the principle has been demonstrated although several problems remain to be solved including the viscous and capacitive coupling between tines and proof that the electronics problems have been solved and high sensitivity can be achieved.

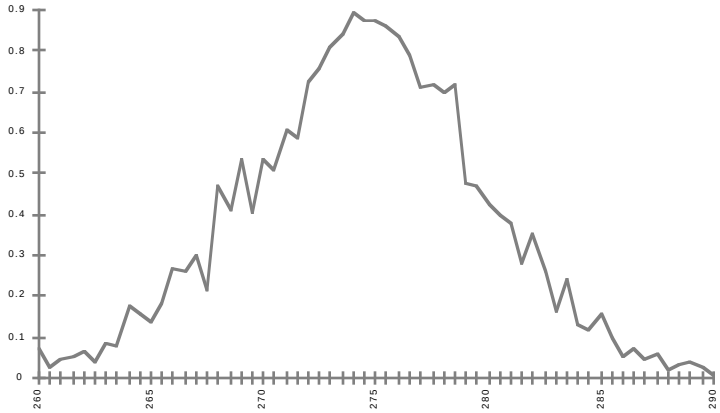

Fig. 14. CTAR module frequency response around the resonance point.

5. STATUS AND PLANS

We are in the process of designing a new micromachined tine array and a new prototype CTAR module using the results of the testing of the laboratory optical interferometry readout device and the results of the tests of the previous CTAR prototype. The new tine array will utilize slightly wider tines with large gaps between tines and we will test an array with grounded barriers between tines to determine if the capacitive coupling can be reduced. Also the tine lengths will be varied so that the resonant frequencies of adjacent tines will differ by at least a factor of 2.5. With these changes and with correction of electronics design errors we expect to complete a sensitive, low-power, high-resolution acoustic spectrometer that can be integrated into a highly sophisticated acoustic detection sensor and target classifier system.

ACKNOWLEDGMENT

This work was performed under the auspices of the U.S. Department of Energy by the Lawrence Livermore National Laboratory under Contract #W-7405-Eng-48, for the U.S. Department of Energy, Office of Nonproliferation and National Security, Office of Research and Development (DOE/NN-20) as part of the Modular Integrated Monitoring System (MIMS) Program and was also supported in part by the U.S. Department of Defense Advanced Research Projects Agency (ARPA) as part of the Internetted Unattended Ground Sensor program. The author would like to acknowledge the contributions of the following people for their efforts on the Acoustic Spectrometer Project: Sang Sheem, Michael Doty, John Cornish, Dean Rippee, Conrad Yu, Dino Ciarlo, David W. Myers and David Fuess.